

DiffSim: Taming Diffusion Models for Evaluating Visual Similarity

Yiren Song* Xiaokang Liu* Mike Zheng Shou†
Show Lab, National University of Singapore

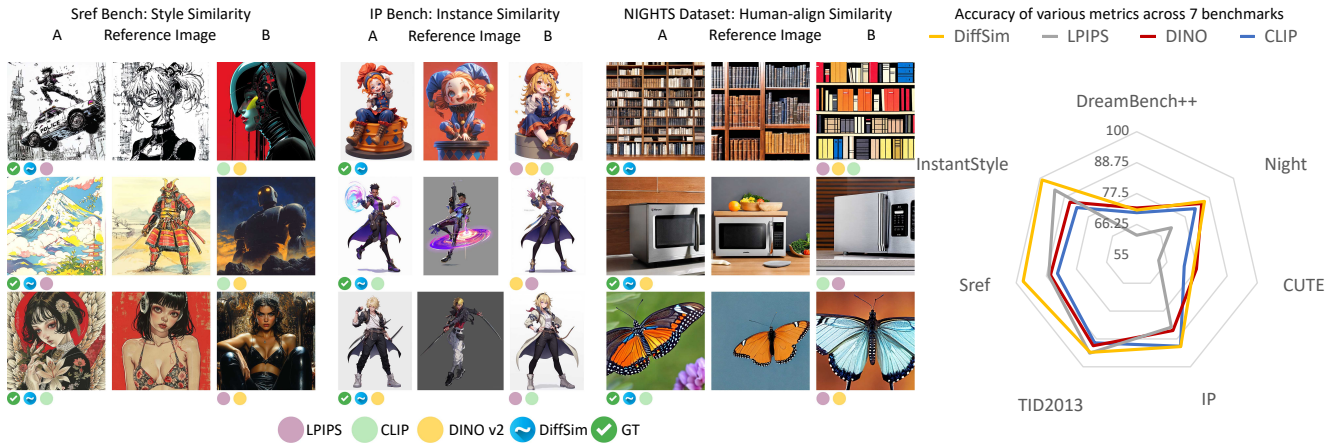


Figure 1. We propose DiffSim, a method that utilizes pre-trained diffusion models to extract image features for evaluating visual similarity. Our method leads in human judgment consistency, style similarity, and instance-level consistency.

Abstract

Diffusion models have fundamentally transformed the field of generative models, making the assessment of similarity between customized model outputs and reference inputs critically important. However, traditional perceptual similarity metrics operate primarily at the pixel and patch levels, comparing low-level colors and textures but failing to capture mid-level similarities and differences in image layout, object pose, and semantic content. Contrastive learning-based CLIP and self-supervised learning-based DINO are often used to measure semantic similarity, but they highly compress image features, inadequately assessing appearance details. This paper is the first to discover that pretrained diffusion models can be utilized for measuring visual similarity and introduces the DiffSim method, addressing the limitations of traditional metrics in capturing perceptual consistency in custom generation tasks. By aligning features in the attention layers of the denoising U-Net, DiffSim evaluates both appearance and style similarity,

showing superior alignment with human visual preferences. Additionally, we introduce the Sref and IP benchmarks to evaluate visual similarity at the level of style and instance, respectively. Comprehensive evaluations across multiple benchmarks demonstrate that DiffSim achieves state-of-the-art performance, providing a robust tool for measuring visual coherence in generative models. Code is released at <https://github.com/showlab/DiffSim>.

1. Introduction

Assessing the consistency of appearance and style between customized generation results and reference images is an important issue. Some studies [34, 59] resort to time-consuming user studies as a supplementary evaluation, despite questions about their fairness and objectivity. Existing evaluation metrics such as CLIP-Image score [37] and DINO score [6], while commonly used, often fail to reflect subtle differences due to their reliance on high-dimensional semantic features for cosine similarity computation. Research [12] indicates that these metrics sometimes do not align with human subjective evaluations and are insufficient for comprehensively measuring consistency in appearance

*Equal contribution.

†Corresponding author.

and style details in generation tasks. Some studies propose human-aligned similarity assessment methods [12], which collect data on human choices of similarity triplets and train models, but their generalization ability in out-of-domain scenarios is considered limited. To overcome these challenges, there is an urgent need for more effective image similarity evaluation metrics in the image generation field.

The motivation of this paper is to assess visual similarity using pre-trained diffusion models. Our rationale is based on three key insights: 1. ReferenceNet [23, 46, 52], uses U-Net to extract features from reference images and directly concatenates these features (K map, V map) in the denoising U-Net’s self-attention layer, effectively maintaining appearance similarity. 2. Custom diffusion [28] demonstrates that the to K and to V matrices in the cross-attention layer are critical modules for stable diffusion models to learn concepts. 3. IP-Adapter [53] injects IP tokens into the cross-attention layer, achieving consistent imagery generation. Since the features of these layers are crucial for generating samples with consistent visual appearance, we believe these features represent the visual appearance and concepts and can be used to assess visual similarity. Recent studies have utilized pre-trained diffusion models for perception tasks [11, 45, 55], demonstrating the potential of generative models in perception tasks and the universality of diffusion model features.

However, two design challenges arise: (1) U-Net, trained on noisy images for denoising purposes, requires noise to be added to the input images (simulating forward diffusion) before feature extraction. (2) Unlike CLIP and DINO, which use high-dimensional semantic features for cosine similarity, Stable Diffusion U-Net’s features are densely packed with spatial information, leading to misalignment at the pixel level. Therefore, simple MSE or cosine calculations between feature maps are impractical, as validated by our subsequent experiments. To address this, we introduce the Aligned Attention Score (AAS), which innovatively uses attention mechanisms to align features of images A and B in the self-attention layer of U-Net, and then calculates the cosine distance between the aligned features.

Furthermore, we explore the variations in features across different layers and denoising timesteps within the denoising U-Net. We find that shallower layers and higher denoising timesteps are suitable for evaluating low-level and style similarities, while deeper layers and lower timesteps excel at assessing semantic similarity. This implies that DiffSim can achieve different similarity measurements with simple configuration adjustments. Besides calculating similarity in the self-attention layers, we also explored using IPAdapter-Plus in the cross-attention layers to evaluate visual similarity. Additionally, we discovered that this technique can be generalized to enhance other architectures such as CLIP and DINO, introducing the CLIP AAS metric and DINO ASS

metric, which significantly improved performance in certain tasks.

Extensive evaluations across multiple benchmarks have proven the effectiveness and advancement of DiffSim. Despite its seemingly straightforward approach, DiffSim excels in all tasks without any additional fine-tuning or supervision, surpassing both CLIP and DINO v2. Remarkably, our experiments reveal that DiffSim’s assessments of image similarity are highly consistent with human judgments, ranking at the forefront in two human consistency benchmarks. Furthermore, DiffSim performs exceptionally well on synthetic images, achieving the best results in style similarity and appearance consistency assessments on our newly proposed Style-ref and IP-ref benchmarks.

We summarize our main contributions as follows:

- We introduce DiffSim, an innovative image similarity assessment method that utilizes the denoising U-Net of pre-trained diffusion models to evaluate visual similarity without the need for additional fine-tuning or specific data supervision.
- We propose the Aligned Attention Score, which precisely aligns image features through attention mechanisms, effectively addressing alignment and information loss issues in traditional assessments, and enables multi-dimensional similarity measurements based on the characteristics of different layers and denoising timesteps in diffusion models.
- We introduce two new benchmarks—Sref and IP bench—to assess style and instance consistency. Extensive experiments and evaluations demonstrate the effectiveness and advancement of DiffSim, which not only surpasses existing CLIP and DINO models but also aligns closely with human visual assessment.

2. Related Work

2.1. Diffusion Models

Diffusion probability models [20, 43] are advanced generative models that restore original data from pure Gaussian noise by learning the distribution of noisy data at various levels of noise. Their powerful capability to adapt to complex data distributions has led diffusion models to achieve remarkable success across several domains including image synthesis [33, 38], image editing [5, 19, 61, 62], and video generation [4, 16, 44]. Stable Diffusion [38] (SD), a notable example, utilizes a U-Net architecture and extensively trains on large-scale text-image datasets to iteratively generate images with impressive text-to-image capabilities. Enhancements in controllable image generation have been driven by methods such as ControlNet [56] and T2I-adapter [30], which significantly improve controllability over generated images by employing multimodal inputs such as depth maps and segmentation maps.

Customized generation methods enable flexible cus-

tomization of concepts and styles by fine-tuning U-Net [39] or certain parameters [22, 28], alongside trainable tokens. Training-free customization methods [48, 49, 53, 59, 60] leverage pre-trained CLIP [37] or Arcface [10] encoders to extract image features. These features are then injected into the cross-attention layers of U-Net through adapter structures for efficient generation. Methods like ReferenceNet [23, 52] integrate reference image features into the self-attention layer of a denoising U-Net, showing advantages in maintaining appearance similarity. These are widely applied in tasks such as image editing [61, 62], facial and body animation [23, 52], and Image2Video tasks [15, 58].

Additionally, recent research has shown that pre-trained diffusion models can also address perception tasks such as 3D awareness [11], keypoint matching [45], and image classification [7]. This paper demonstrates the practicality and technical maturity of using pre-trained diffusion models for image similarity assessment.

2.2. Perceptual Similarity

Traditional metrics such as Manhattan l_1 , Euclidean l_2 , Mean Squared Error (MSE), and Peak Signal-to-Noise Ratio (PSNR) use point-to-point differences to measure similarity, but lack the ability to effectively understand the global structure and content of images. In contrast, deep learning-based metrics that utilize features extracted from pretrained networks like VGG [41] and AlexNet [27] have proven superior. Further improvements in these metrics have been achieved through optimizations on perceptual data, as seen in methods like LPIPS [57], PIE-APP [36], and DreamSim [12]. Research by Muttenthaler [31] on concept similarity within a subset of the THINGS dataset [18] provides insights into high-level human similarity.

Meanwhile, DreamSim [12] integrates features from models like CLIP [37] and DINO [32], trained on synthetic datasets and human annotations, to achieve state-of-the-art results. However, CLIP and DINO encode images into 1×768 -dimensional feature vectors for cosine similarity computation, emphasizing categorical attributes over fine-grained appearance similarity. This high compression sometimes leads to divergences from human perception, indicating a need for more effective visual similarity metrics in the generative AI and metric learning fields.

2.3. Style Similarity Evaluation

Artistic style is often defined as a collection of global characteristics associated with an artist or artistic movement, encompassing elements like color usage, brushstroke techniques, composition, and perspective. Early algorithms modeled style using low-level visual features [24, 40], while modern approaches predominantly utilize neural networks for style transfer and classification tasks. For instance, Gatys et al. [14] utilized Gram matrices as style descriptors, while Luan et al. [29] introduced a photorealism reg-

ularization term to optimize style transfer. Recently, Wang et al. [50] developed a style recognition model based on synthetic style pairs, and CSD [42] introduces a multi-label contrastive learning scheme to extract style descriptors.

In the era of generative AI, techniques like the LoRA model [21] can generate new samples consistent with a few trained style images, or methods like IP-Adapter [54] and InstantStyle [48] directly obtain style representations. When combined with text prompts, these technologies can create entirely new artistic styles, adding complexity and ambiguity. This diversity in style poses challenges for style similarity evaluation, demanding methods that more finely capture and understand stylistic relationships between images. To address this, our proposed DiffSim method leverages the diffusion model trained on massive image-text pairs, enabling advanced style similarity assessment without any fine-tuning.

3. Method

DiffSim leverages the implicit alignment mechanism of attention to align two images at the style or semantic level, followed by similarity computation. In Sec. 3.1, we briefly review the attention mechanism in the Stable Diffusion model. Sec. 3.2 introduces the mechanism for calculating AAS (Aligned Attention Score) within a single attention layer. Sec. 3.3 provides a detailed explanation of how DiffSim is computed using pretrained models and AAS. Sec. 3.4 introduce two benchmark we propose.

3.1. Preliminaries

3.1.1. Cross Attention in Diffusion Model

Taking Stable Diffusion as an example, cross-attention layers play a crucial role in fusing images and texts, allowing diffusion models to generate images that are consistent with textual descriptions. The cross-attention layer receives the query, key, and value matrices, i.e., Q_{cross} , K_{cross} , and V_{cross} , from the noisy image and prompt. Specifically, Q_{cross} is derived from the spatial features of the noisy image $\phi_{\text{cross}}(z_t)$ by learned linear projections ℓ_q , while K_{cross} and V_{cross} are projected from the textual embedding P_{emb} of the input prompt P using learned linear projections denoted as ℓ_k and ℓ_v , respectively. The cross-attention map is defined as:

$$Q_{\text{cross}} = \ell_q(\phi_{\text{cross}}(z_t)), \quad (1)$$

$$K_{\text{cross}} = \ell_k(P_{\text{emb}}), \quad (2)$$

$$M_{\text{cross}} = \text{Softmax} \left(\frac{Q_{\text{cross}} K_{\text{cross}}^T}{\sqrt{d_{\text{cross}}}} \right), \quad (3)$$

where d_{cross} is the dimension of the keys and queries. The final output is defined as the fused feature of the text and image, denoted as $\hat{\phi}(z_t) = M_{\text{cross}} V_{\text{cross}}$, where $V_{\text{cross}} = \ell_v(P_{\text{emb}})$. Intuitively, each cell in the cross-attention map,

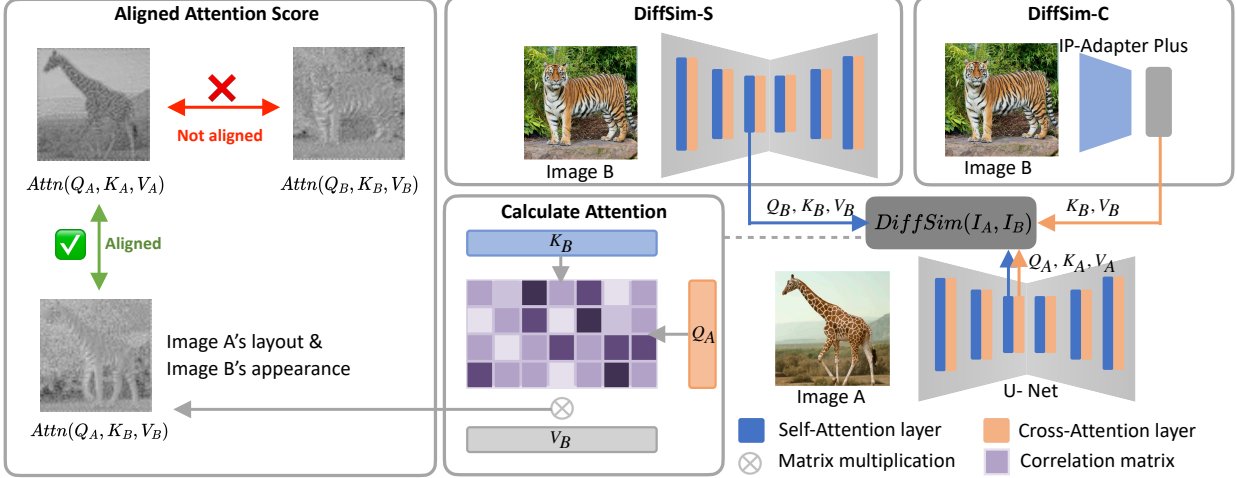


Figure 2. The illustration shows two DiffSim implementations: DiffSim-S using self-attention, where U-Net extracts features from both images to compute Aligned Attention Score (AAS) at a specified layer; and DiffSim-C using cross-attention, where features are extracted via IP-Adapter Plus and U-Net with swapped image inputs.

denoted as M_{ij} , determines the weights attributed to the value of the j -th token relative to the spatial feature i of the image. The cross-attention map enables the diffusion model to locate/align the tokens of the prompt in the image area.

3.1.2. Self Attention in Diffusion Model

Unlike cross-attention, the self-attention layer receives the keys matrix K_{self} and the query matrix Q_{self} from the noisy image $\phi_{\text{self}}(z_t)$ through learned linear projections $\bar{\ell}_K$ and $\bar{\ell}_Q$, respectively. The self-attention map is defined as:

$$Q_{\text{self}} = \bar{\ell}_q(\phi_{\text{self}}(z_t)), \quad (4)$$

$$K_{\text{self}} = \bar{\ell}_K(\phi_{\text{self}}(z_t)), \quad (5)$$

$$M_{\text{self}} = \text{Softmax}\left(\frac{Q_{\text{self}}K_{\text{self}}^T}{\sqrt{d_{\text{self}}}}\right), \quad (6)$$

where d_{self} is the dimension of K_{self} and Q_{self} . M_{self} determines the weights assigned to the relevance of the i -th and j -th spatial features in the image and can affect the spatial layout and shape details of the generated image. Consequently, the self-attention map can be utilized to preserve the spatial structure characteristics of the original image throughout the image editing process.

3.2. Aligned Attention Score

In this section, we introduce the Aligned Attention Score (AAS), a new metric designed to provide implicit alignment between images while measuring various aspects such as semantic content and style. Traditional similarity assessment methods, such as Mean Squared Error (MSE) or cosine similarity, often assume that the latent features of images are pixel-aligned. However, this assumption frequently

fails in practical applications due to significant changes in style, pose, or context, leading to poor and inaccurate similarity measurements. Moreover, popular methods like CLIP and DINO compress high-dimensional block features into a lower-dimensional feature space using Multilayer Perceptrons (MLPs) and compute cosine similarity on these simplified representations. While effective at semantic-level comparisons, this compression process can result in the loss of critical detail, failing to capture subtle differences vital for some applications.

AAS addresses misalignment issues by leveraging attention mechanisms in pretrained U-Net or Transformer-based models. We define L_A and L_B as the latent representations of images I_A and I_B respectively. AAS dynamically aligns these representations using the neural network’s attention function $\text{attn}(Q, K, V)$:

$$\text{AAS}(L_A, L_B) = \cos(\text{attn}(Q_A, K_A, V_A), \text{attn}(Q_A, K_B, V_B)), \quad (7)$$

$$\text{AAS}(L_B, L_A) = \cos(\text{attn}(Q_B, K_B, V_B), \text{attn}(Q_B, K_A, V_A)). \quad (8)$$

By aligning dense latent representations in the attention layers, AAS ensures that each image’s features are evaluated both as queries and keys against the features of the other image. This method not only compensates for the lack of pixel alignment but also preserves the richness of the feature space, providing a more accurate method of measuring perceptual similarity that closely aligns with human visual judgment:

$$\text{Similarity}(L_A, L_B) = \text{AAS}(L_A, L_B) + \text{AAS}(L_B, L_A). \quad (9)$$

This integrated approach to image alignment and similarity assessment leverages different granularity representations provided by pretrained models, effectively improving the handling of image misalignment and information loss.

3.3. DiffSim Metric

To fully utilize the attention mechanisms in stable diffusion, we repurpose its self-attention and cross-attention for our AAS, forming two methods: DiffSim-S and DiffSim-C.

3.3.1. DiffSim-S

It is well known that the features in the U-Net’s self-attention layers can reflect the consistency of image appearance. Previous works [8, 9, 17, 23, 46, 47, 51, 52, 58, 61, 62] have utilized this characteristic to achieve high-consistency image and video generation.

In the aforementioned methods, the embedding of features in the self-attention layers enables the generation of images or videos with appearance consistency. Thus, we posit that the features in the U-Net’s self-attention layers can reflect the consistency of image appearance. We propose an implementation of the self-attention layers in DiffSim. We calculate:

$$\text{DiffSim-S}(I_A, I_B, n, t) = \frac{1}{2} \left(\text{AAS}(z_{t,\text{self},n}^A, z_{t,\text{self},n}^B) + \text{AAS}(z_{t,\text{self},n}^B, z_{t,\text{self},n}^A) \right), \quad (10)$$

where $z_{t,\text{self},n}^A$ and $z_{t,\text{self},n}^B$ denote the latent representations of images I_A and I_B within the n -th self-attention layer of the U-Net at denoising timestep t , respectively.

3.3.2. DiffSim-C

The Stable diffusion enhances text-to-image generation by integrating text embeddings as conditions within its cross-attention layers. Prior studies [3, 28] have highlighted the pivotal role of these layers in learning customized model concepts, demonstrating that new concepts can be learned through mere fine-tuning of these layers. Given this context, we explored the potential of cross-attention layer features to assess image similarity. However, traditionally, cross-attention layers only support the calculation of attention between image latents and text embeddings. To extend their capability, we employed IP-Adapter Plus [53], which utilizes patch features from the CLIP image encoder and increases the number of IP tokens to 16, injecting these tokens into the cross-attention layers of U-Net. This setup facilitates a more nuanced computation of attention that involves interaction between image latents and enhanced IP tokens.

We designed the structure illustrated in Figure 2, where Image I_A and Image I_B are input into IP-Adapter Plus and the denoising U-Net, respectively. The attention-based similarity scores are then computed by comparing the latents of one image to the IP tokens derived from the other, and vice

versa. Specifically, we calculate:

$$\text{DiffSim-C}(I_A, I_B, n, t) = \frac{1}{2} \left(\text{AAS}(z_{t,\text{cross},n}^A, IP_B) + z_{t,\text{cross},n}^B, IP_A \right), \quad (11)$$

where $z_{t,\text{cross},n}^A$ and $z_{t,\text{cross},n}^B$ denote the latent representations of Images I_A and I_B within the n -th cross-attention layer of the U-Net at denoising timestep t , respectively. Similarly, IP_A and IP_B represent the IP tokens associated with Images I_A and I_B , respectively.

3.3.3. DiffSim Adaptation to Various Frameworks

The DiffSim method is widely applicable and allows for the analysis of image features by computing feature similarity in the attention layers. We have extended the DiffSim approach to the CLIP Image Encoder and DINO v2 architectures. CLIP trains image and text encoders through contrastive learning to understand the relationship between images and text, aiming to maximize the similarity of matching image-text pairs, typically using Vision Transformer or ResNet as the image encoder. DINO operates in a self-supervised manner with a teacher-student network architecture, both utilizing Vision Transformers. The student network learns visual representations by mimicking the output of the teacher network, which has been augmented with random data transformations. The teacher network is updated through exponential moving average (EMA). For specific self-attention layers in the CLIP and DINO v2 models, we calculate AAS and introduce new metrics, CLIP AAS and DINO v2 AAS.

3.4. New Benchmarks

3.4.1. Sref Bench

Style is subjective, thus an effective style similarity metric should align with human perceptions and definitions of style. Therefore, we have collected 508 styles, each hand-picked by human artists and featuring four thematically distinct reference images, created using Midjourney’s Sref mode [1]. Midjourney’s style reference feature allows users to guide the style or aesthetic of generated images by using external pictures or style seeds in their prompts. Figure 12 shows some examples in our benchmark.

3.4.2. IP Bench

Instance-level consistency is one of the primary tasks in customized generation. However, there is a lack of high-quality benchmarks for assessing character consistency. We have collected images of 299 IP characters and used advanced Flux models [2] and the IP-Adapter to create several variants of each character with different consistency weights.

4. Experiment

4.1. Experimental Setting

We implemented DiffSim based on Stable Diffusion 1.5, where the total time step T for the SD diffusion model is



Figure 3. To evaluate style similarity and instance-level similarity, we introduced the Sref bench and IP bench. The Sref dataset contains 508 styles, each generated by Midjourney’s sref mode and handpicked by human artists, represented through four different thematic reference images. The IP dataset includes a set of 299 IPs comprising highly similar images along with variants that gradually decrease in similarity.

1000. U-Net includes downsampling blocks, middle blocks, and upsampling blocks. We explore using features from both downsampling and upsampling blocks. We also conducted grid searches across different layers and denoising time steps for each task, reporting the best results among these choices; further details are provided in the supplementary materials. The default setting of DiffSim is using the self-attn layer, and the input image resolution of 512×512 .

4.2. Baselines

We compare five similarity assessment methods as baselines, including CLIP [37], DINO v2 [32], as well as LPIPS [57], Foreground Feature Averaging (FFA) [26], and the Gram metric [13] for style similarity assessment. All baseline methods used for comparison are implemented based on pre-trained models, ensuring a fair representation of the inherent performance differences in similarity metrics among foundational models. Methods involving fine-tuning on human-rated datasets [12] are excluded from our comparison. Additionally, we demonstrate that an ensemble of CLIP, DINO v2 and DiffSim using a hard vote approach can improve performance.

4.3. Benchmarks

In addition to using the Sref bench and IP bench we proposed, we also employed 6 existing benchmarks.

NIGHTS Perceptual Dataset. The NIGHTS[12] (Novel Image Generations with Human-Tested Similarities) dataset comprises 20,019 image triplets, each containing a reference image and two distortions, evaluated for perceptual similarity by human observers. The dataset was generated using Stable Diffusion 2.1 with prompts from categories across prominent datasets like ImageNet and CIFAR.

TID2013. The TID2013[35] (Tampere Image Database 2013) dataset contains 3,000 test images derived from 25 reference images, each subjected to 24 types of distortions, producing 120 distorted images per reference. These distortions encompass a range of realistic noise and artifacts intended to evaluate image quality assessment metrics.

CUTE Benchmark. CUTE[26] includes 18,000 images of 180 objects across 50 categories under varied conditions to

test intrinsic object-centric similarity. It features objects in diverse poses and settings, providing a robust resource for benchmarking similarity metrics in varying visual contexts.

Dreambench++. Dreambench++[34] serves as a human-aligned, automated benchmark for personalized image generation model evaluation, focusing on concept preservation and prompt adherence. It utilizes multimodal GPT models aligned with human preferences, with a refined rating system for efficient method comparison.

InstantStyle Benchmark. InstantStyle[48] is an advanced method for style customization. We have organized 30 styles on the InstantStyle project homepage, each including 5 images, to serve as a supplementary benchmark for style evaluation.

TikTok Dataset. The TikTok[25] dataset includes 300 dance videos (10-15 seconds), which we use to assess video appearance consistency in this paper.

4.4. Quantitative Evaluation

We employ the same evaluation protocol as previous methods [12]. Similarity scores are computed between a reference image and two candidate images. Image with the higher score is selected as the choice of current evaluated model, and we tally the accuracy of correctly classified selections for each metric model. The accuracy results of each metric across all benchmarks are displayed in the Table 1. The selection of candidate images varies slightly for different benchmarks; for further details, please refer to the supplementary materials.

Human Perceptual Consistency Assessment. To evaluate the overall similarity and consistency between DiffSim and human judgments, we conducted experiments on the NIGHTS and Dreambench++ benchmarks. As seen in Table 1, DiffSim achieved the best performance on the Nights dataset, while on the Dreambench dataset, its performance is comparable to that of the top-performing DINO v2.

Instance Similarity Assessment. To compare the accuracy of instance-level metrics, experiments were conducted on the CUTE and IP benchmarks. On the CUTE dataset, DINO v2 and FFA take the lead, but their performance does not

Table 1. Performance of different metrics across various benchmarks. Best results are highlighted in red and second-best in blue (excluding ensemble model). The ensemble model takes predictions from CLIP, DINO v2 and DiffSim and determines the final classification based on the majority rule. Results showing improvements over the original three methods in the ensemble model are highlighted in bold.

Model / Benchmark	Human-align Similarity		Instance Similarity		Low-level Similarity	Style Similarity	
	NIGHTS	Dreambench++	CUTE	IP	TID2013	Sref	InstantStyle bench
LPIPS[57]	71.13%	62.33%	63.17%	84.01%	94.50%	87.85%	93.15%
Gram[13]	-	-	-	-	-	84.05%	88.30%
CLIP[37]	82.26%	70.54%	72.71%	91.70%	90.33%	84.60%	82.90%
DINO v2[32]	85.24%	72.25%	77.27%	85.35%	91.50%	87.20%	86.10%
FFA[26]	77.78%	65.21%	76.55%	89.70%	75.17%	62.55%	60.65%
CLIP AAS (ours)	82.18%	67.23%	71.78%	88.03%	96.33%	94.45%	97.80%
DINO v2 AAS (ours)	86.47%	70.01%	77.04%	90.38%	95.83%	95.90%	96.65%
DiffSim (ours)	86.52%	71.50%	76.17%	91.84%	94.17%	97.40%	99.05%
Ensemble	89.43%	72.15%	77.78%	94.92%	95.00%	91.70%	88.30%

Table 2. Evaluation of different DiffSim architectures. The best results are highlighted in bold.

Setting	DiffSim-S SD1.5	DiffSim-C SD1.5	DiffSim-S SD-XL
NIGHTS	86.52%	79.16%	78.05%
Dreambench++	71.50%	67.45%	63.93%
CUTE	72.06%	76.17%	69.94%
IP	92.04%	77.06%	83.41%
TID2013	94.17%	94.00%	91.33%
Sref	97.40%	94.70%	93.05%
InstantStyle	99.05%	95.10%	96.55%

surpass DiffSim by a large margin. On the IP benchmark, DiffSim leads with a significant margin. It shows that DiffSim is capable to capture instance level similarity.

Low-level Similarity Assessment. To evaluate the accuracy of various methods, experiments were also conducted on the TID2013 dataset. The DiffSim method showed considerable versatility, achieving excellent performance in low-level similarity assessment merely by modifying the denoising time step, far surpassing CLIP and DINO v2, and comparable to LPIPS.

Style Similarity Assessment. To assess the accuracy of style similarity metrics, experiments were conducted on the Sref bench and InstantStyle bench. Across these two benchmarks, DiffSim achieved the best results, demonstrating its strong ability in evaluating stylish similarity.

Appearance Consistency Assessment in Video. Temporal appearance consistency is crucial for assessing video generation and video-to-image models. An ideal metric should be unaffected by changes in object position and layout, ensuring stable similarity scores across frames of the same subject, regardless of movement. We evaluate on the TikTok dataset by measuring variance of different similarity scores between the first frame and other frames. As shown in Table 4, our CLIP AAS outperforms others, with CLIP and DiffSim yielding similar results.

Table 3. Ablation study. CLIP and DINO v2 features (both AAS and original) are all extracted from the last layer.

Benchmark	Metrics			Variance ↓
	Sref	IP	NIGHTS	
DiffSim	97.40%	92.04%	86.82%	LPIPS 3.565e-3
Diffusion feature	78.80%	62.47%	66.75%	CLIP 1.007e-3
CLIP AAS	71.15%	87.36%	80.54%	DINO v2 6.340e-3
CLIP features	66.50%	82.54%	75.84%	FFA 4.381e-3
DINO v2 AAS	78.50%	90.38%	86.41%	CLIP AAS 4.397e-7
DINO v2 feature	76.90%	87.56%	81.00%	DINO v2 AAS 1.825e-3
				DiffSim 1.335e-3

CLIP AAS and DINO v2 AAS Assessment As indicated in the Table 1 and 4, CLIP AAS and DINO v2 AAS show largely comparable results to CLIP and DINO v2, with some improvements on specific benchmarks. This further demonstrates the effectiveness of the proposed AAS and its scalability across various attention-based frameworks.

Ensemble Model We show that by ensembling CLIP, DINO v2 and DiffSim models through hard vote, the performance has shown an improvement over three original methods across several benchmarks. This demonstrates that DiffSim can be used to compensate for the limitations of the CLIP and DINO v2 models.

4.5. Performance Analysis

In this section, we select three representative benchmarks to demonstrate the key factors affecting DiffSim’s performance in three similarity evaluation tasks.

Denoising Timestep. Our observations reveal that diffusion models manifest distinct characteristics at different denoising timesteps. As shown in Figure 5, higher t values (900) cater to style assessments with rich low-level features, while lower t values (500) excel in instance-level similarity tasks on the NIGHTS dataset.

Different Attention Blocks. Results from IP bench and NIGHTS dataset show that layers near the middle of the Unet (Down sample layer 2, Up sample layer 0) focus more

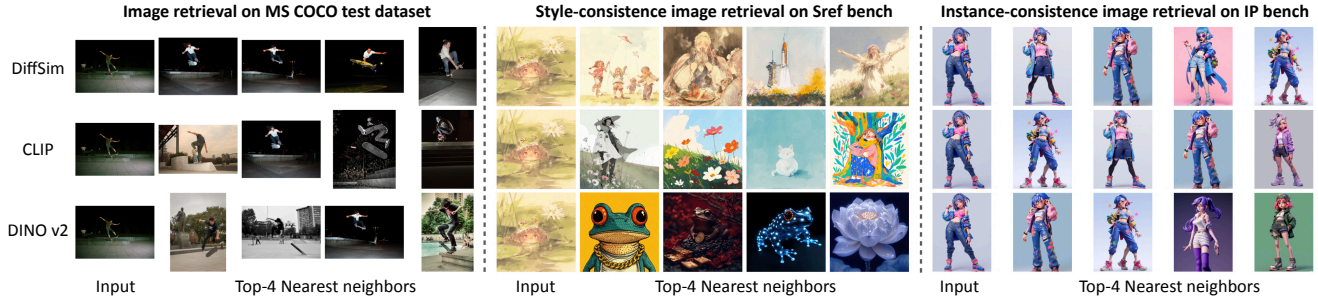


Figure 4. Some retrieval examples using DiffSim, CLIP, and DINO v2. The left, middle and right column displays retrieval results from the Sref benchmark, MS COCO Test dataset and the IP benchmark respectively.

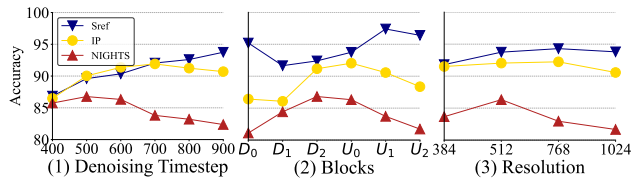


Figure 5. Evaluation of different benchmarks across different timesteps, blocks and resolutions. (1) All experiments across timesteps are conducted on the U_0 block of SD 1.5. (2) The results of different blocks of Sref, IP, and NIGHTS experiments are completed with fixed t of 900, 750, and 600, respectively. (3) The results of different resolutions are all based on the best settings of timesteps and blocks.

on instance level, while those closer to the ends of the network (Down sample layer 0, Up sample layer 1) excel on the Sref bench. We believe that shallow features are more advantageous for assessing style similarity.

Resolution. We test resolutions from 384 to 1024, with no notable impact across most datasets. However, increasing the resolution from 512 to 768 slightly improves performance on the IP and Sref benches due to their original higher resolution, unlike the NIGHTS dataset, which did not benefit from higher inference resolutions. We standardize the resolution at 512x512 to align with Stable Diffusion 1.5’s training settings.

Different DiffSim Architectures. Table 2 demonstrates the impact of different DiffSim architectures. Overall, DiffSim-S SD1.5 shows superior performance. For instance-level similarity assessments on the CUTE dataset, DiffSim-C SD1.5 performs slightly better.

4.6. Ablation Study

In this section, we present the results of ablation studies to demonstrate the effectiveness of the key design introduced in this paper, the Aligned Attention Score (AAS). For comparison, we fix the layer and timestep setting, directly calculating the cosine similarity of latent diffusion model features, CLIP features and DINO v2 features L_A , L_B . As shown in Table 3, the results significantly deteriorate when

AAS feature alignment is not used.

4.7. Image Retrieval

To further analyze DiffSim’s performance, we conduct image retrieval experiments on the Sref bench, IP bench, and MS COCO Test dataset, with Figure 4 showcasing the top 4 nearest neighbors. During style consistency retrieval on the Sref bench, our results are quite precise, while baseline methods are often influenced by image category attributes. On the COCO Test dataset, our retrieval results focus not only on semantics but also on background similarity, which is better than the baseline methods. On the IP bench, our results are more precise. Please refer to the supplementary materials for more retrieval examples.

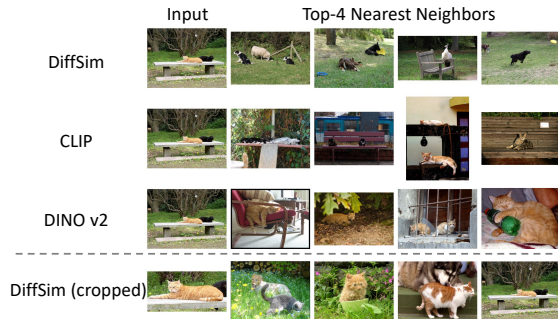


Figure 6. Failure case.

4.8. Limitation and Failure Case

DiffSim occasionally overemphasizes background features, neglecting key subject details, especially in images with smaller subjects. As shown in Figure 6, DiffSim retrieves images of dogs with similar backgrounds using an image of cats. Cropping the subject can mitigate this issue.

5. Conclusion

This paper introduces DiffSim, marking the first application of diffusion models in image similarity assessment. DiffSim calculates the Aligned Attention Score in the self-attention or cross-attention layers of Stable Diffusion, effectively evaluating visual similarity and demonstrating high alignment with human perception across various tasks. By

exploring the characteristics of different layers and denoising steps within diffusion models, DiffSim achieves accurate assessments of human-aligned, instance-level, and style similarity. Extensive experiments on multiple benchmark datasets confirm the effectiveness of DiffSim, providing an efficient tool for evaluating visual consistency.

References

- [1] Midjourney sref: Prompt library and examples. <https://midjourneysref.com/discover?page=1>. Accessed: 2024-11-21. **5**
- [2] Flux.1 AI. Flux.1 ai, 2024. **5**
- [3] Yuval Alaluf, Daniel Garibi, Or Patashnik, Hadar Averbuch-Elor, and Daniel Cohen-Or. Cross-image attention for zero-shot appearance transfer. In *ACM SIGGRAPH 2024 Conference Papers*, pages 1–12, 2024. **5**
- [4] Andreas Blattmann, Tim Dockhorn, Sumith Kulal, Daniel Mendelevitch, Maciej Kilian, Dominik Lorenz, Yam Levi, Zion English, Vikram Voleti, Adam Letts, et al. Stable video diffusion: Scaling latent video diffusion models to large datasets. *arXiv preprint arXiv:2311.15127*, 2023. **2**
- [5] Tim Brooks, Aleksander Holynski, and Alexei A Efros. Instructpix2pix: Learning to follow image editing instructions. In *Proceedings of the IEEE/CVF Conference on Computer Vision and Pattern Recognition*, pages 18392–18402, 2023. **2**
- [6] Mathilde Caron, Hugo Touvron, Ishan Misra, Hervé Jégou, Julien Mairal, Piotr Bojanowski, and Armand Joulin. Emerging properties in self-supervised vision transformers. 2021 *ieee*. In *CVF International Conference on Computer Vision (ICCV)*, 2021. **1**
- [7] Huanran Chen, Yinpeng Dong, Zhengyi Wang, Xiao Yang, Chengqi Duan, Hang Su, and Jun Zhu. Robust classification via a single diffusion model. *arXiv preprint arXiv:2305.15241*, 2023. **3**
- [8] Xi Chen, Zhiheng Liu, Mengting Chen, Yutong Feng, Yu Liu, Yujun Shen, and Hengshuang Zhao. Livephoto: Real image animation with text-guided motion control. *arXiv preprint arXiv:2312.02928*, 2023. **5**
- [9] Zhiyuan Chen, Jiajiong Cao, Zhiquan Chen, Yuming Li, and Chenguang Ma. Echomimic: Lifelike audio-driven portrait animations through editable landmark conditions. *arXiv preprint arXiv:2407.08136*, 2024. **5**
- [10] Jiankang Deng, Jia Guo, Niannan Xue, and Stefanos Zafeiriou. Arcface: Additive angular margin loss for deep face recognition. In *Proceedings of the IEEE/CVF conference on computer vision and pattern recognition*, pages 4690–4699, 2019. **3**
- [11] Mohamed El Banani, Amit Raj, Kevis-Kokitsi Maninis, Abhishek Kar, Yuanzhen Li, Michael Rubinstein, Deqing Sun, Leonidas Guibas, Justin Johnson, and Varun Jampani. Probing the 3d awareness of visual foundation models. In *Proceedings of the IEEE/CVF Conference on Computer Vision and Pattern Recognition*, pages 21795–21806, 2024. **2, 3**
- [12] Stephanie Fu, Netanel Tamir, Shobhita Sundaram, Lucy Chai, Richard Zhang, Tali Dekel, and Phillip Isola. Dream-sim: Learning new dimensions of human visual similarity using synthetic data. *arXiv preprint arXiv:2306.09344*, 2023. **1, 2, 3, 6**
- [13] Leon A Gatys. A neural algorithm of artistic style. *arXiv preprint arXiv:1508.06576*, 2015. **6, 7**
- [14] Leon A. Gatys, Alexander S. Ecker, and Matthias Bethge. Image style transfer using convolutional neural networks. In *2016 IEEE Conference on Computer Vision and Pattern Recognition (CVPR)*, pages 2414–2423, 2016. **3**
- [15] Xun Guo, Mingwu Zheng, Liang Hou, Yuan Gao, Yufan Deng, Pengfei Wan, Di Zhang, Yufan Liu, Weiming Hu, Zhengjun Zha, et al. I2v-adapter: A general image-to-video adapter for diffusion models. In *ACM SIGGRAPH 2024 Conference Papers*, pages 1–12, 2024. **3**
- [16] Yuwei Guo, Ceyuan Yang, Anyi Rao, Yaohui Wang, Yu Qiao, Dahua Lin, and Bo Dai. Animatediff: Animate your personalized text-to-image diffusion models without specific tuning. *arXiv preprint arXiv:2307.04725*, 2023. **2**
- [17] Xuanhua He, Quande Liu, Shengju Qian, Xin Wang, Tao Hu, Ke Cao, Keyu Yan, Man Zhou, and Jie Zhang. Id-animator: Zero-shot identity-preserving human video generation. *arXiv preprint arXiv:2404.15275*, 2024. **5**
- [18] Martin N Hebart, Adam H Dickler, Alexis Kidder, Wan Y Kwok, Anna Corriveau, Caitlin Van Wicklin, and Chris I Baker. Things: A database of 1,854 object concepts and more than 26,000 naturalistic object images. *PLoS one*, 14(10):e0223792, 2019. **3**
- [19] Amir Hertz, Ron Mokady, Jay Tenenbaum, Kfir Aberman, Yael Pritch, and Daniel Cohen-Or. Prompt-to-prompt image editing with cross attention control. *arXiv preprint arXiv:2208.01626*, 2022. **2**
- [20] Jonathan Ho, Ajay Jain, and Pieter Abbeel. Denoising diffusion probabilistic models. *Advances in neural information processing systems*, 33:6840–6851, 2020. **2**
- [21] Edward J. Hu, Yelong Shen, Phillip Wallis, Zeyuan Allen-Zhu, Yuanzhi Li, Shean Wang, Lu Wang, and Weizhu Chen. Lora: Low-rank adaptation of large language models, 2021. **3**
- [22] Edward J Hu, Yelong Shen, Phillip Wallis, Zeyuan Allen-Zhu, Yuanzhi Li, Shean Wang, Lu Wang, and Weizhu Chen. LoRA: Low-rank adaptation of large language models. In *International Conference on Learning Representations*, 2022. **3**
- [23] Li Hu. Animate anyone: Consistent and controllable image-to-video synthesis for character animation. In *Proceedings of the IEEE/CVF Conference on Computer Vision and Pattern Recognition*, pages 8153–8163, 2024. **2, 3, 5**
- [24] James M. Hughes, Daniel J. Graham, C. Robert Jacobsen, and Daniel N. Rockmore. Comparing higher-order spatial statistics and perceptual judgements in the stylometric analysis of art. In *2011 19th European Signal Processing Conference*, pages 1244–1248, 2011. **3**
- [25] Yasamin Jafarian and Hyun Soo Park. Self-supervised 3d representation learning of dressed humans from social media videos. *IEEE Transactions on Pattern Analysis and Machine Intelligence*, 45(7):8969–8983, 2022. **6**
- [26] Klemen Kotar, Stephen Tian, Hong-Xing Yu, Dan Yamins, and Jiajun Wu. Are these the same apple? comparing images

- based on object intrinsics. *Advances in Neural Information Processing Systems*, 36:40853–40871, 2023. 6, 7
- [27] Alex Krizhevsky, Ilya Sutskever, and Geoffrey E Hinton. Imagenet classification with deep convolutional neural networks. *Advances in neural information processing systems*, 25, 2012. 3
- [28] Nupur Kumari, Bingliang Zhang, Richard Zhang, Eli Shechtman, and Jun-Yan Zhu. Multi-concept customization of text-to-image diffusion. In *Proceedings of the IEEE/CVF Conference on Computer Vision and Pattern Recognition*, pages 1931–1941, 2023. 2, 3, 5
- [29] Fujun Luan, Sylvain Paris, Eli Shechtman, and Kavita Bala. Deep photo style transfer, 2017. 3
- [30] Chong Mou, Xintao Wang, Liangbin Xie, Jian Zhang, Zhong-gang Qi, Ying Shan, and Xiaoju Qie. T2i-adapter: Learning adapters to dig out more controllable ability for text-to-image diffusion models. *arXiv preprint arXiv:2302.08453*, 2023. 2
- [31] Lukas Muttenthaler, Jonas Dippel, Lorenz Linhardt, Robert A Vandermeulen, and Simon Kornblith. Human alignment of neural network representations. *arXiv preprint arXiv:2211.01201*, 2022. 3
- [32] Maxime Oquab, Timothée Darcet, Théo Moutakanni, Huy Vo, Marc Szafraniec, Vasil Khalidov, Pierre Fernandez, Daniel Haziza, Francisco Massa, Alaaeldin El-Nouby, et al. Dinov2: Learning robust visual features without supervision. *arXiv preprint arXiv:2304.07193*, 2023. 3, 6, 7
- [33] William Peebles and Saining Xie. Scalable diffusion models with transformers. In *Proceedings of the IEEE/CVF International Conference on Computer Vision*, pages 4195–4205, 2023. 2
- [34] Yuang Peng, Yuxin Cui, Haomiao Tang, Zekun Qi, Runpei Dong, Jing Bai, Chunrui Han, Zheng Ge, Xiangyu Zhang, and Shu-Tao Xia. Dreambench++: A human-aligned benchmark for personalized image generation. *arXiv preprint arXiv:2406.16855*, 2024. 1, 6
- [35] Nikolay Ponomarenko, Oleg Ieremeiev, Vladimir Lukin, Lina Jin, Karen Egiazarian, Jaakko Astola, Benoit Vozel, Kacem Chehdi, Marco Carli, Federica Battisti, et al. A new color image database tid2013: Innovations and results. In *Advanced Concepts for Intelligent Vision Systems: 15th International Conference, ACIVS 2013, Poznań, Poland, October 28-31, 2013. Proceedings 15*, pages 402–413. Springer, 2013. 6
- [36] Ekta Prashnani, Hong Cai, Yasamin Mostofi, and Pradeep Sen. Pieapp: Perceptual image-error assessment through pairwise preference. In *Proceedings of the IEEE Conference on Computer Vision and Pattern Recognition*, pages 1808–1817, 2018. 3
- [37] Alec Radford, Jong Wook Kim, Chris Hallacy, Aditya Ramesh, Gabriel Goh, Sandhini Agarwal, Girish Sastry, Amanda Askell, Pamela Mishkin, Jack Clark, Gretchen Krueger, and Ilya Sutskever. Learning transferable visual models from natural language supervision. In *Proceedings of the 38th International Conference on Machine Learning*, pages 8748–8763. PMLR, 2021. 1, 3, 6, 7
- [38] Robin Rombach, Andreas Blattmann, Dominik Lorenz, Patrick Esser, and Björn Ommer. High-resolution image synthesis with latent diffusion models. In *Proceedings of the IEEE/CVF conference on computer vision and pattern recognition*, pages 10684–10695, 2022. 2
- [39] Nataniel Ruiz, Yuanzhen Li, Varun Jampani, Yael Pritch, Michael Rubinstein, and Kfir Aberman. Dreambooth: Fine tuning text-to-image diffusion models for subject-driven generation. In *Proceedings of the IEEE/CVF conference on computer vision and pattern recognition*, pages 22500–22510, 2023. 3
- [40] Robert Sablatnig, Paul Kammerer, and Ernestine Zolda. Hierarchical classification of paintings using face- and brush stroke models. *Proc. 14th Int. Conference on Pattern Recognition*, 1, 2002. 3
- [41] Karen Simonyan. Very deep convolutional networks for large-scale image recognition. *arXiv preprint arXiv:1409.1556*, 2014. 3
- [42] Gowthami Somepalli, Anubhav Gupta, Kamal Gupta, Shramay Palta, Micah Goldblum, Jonas Geiping, Abhinav Shrivastava, and Tom Goldstein. Measuring style similarity in diffusion models. *arXiv preprint arXiv:2404.01292*, 2024. 3
- [43] Jiaming Song, Chenlin Meng, and Stefano Ermon. Denoising diffusion implicit models. *arXiv preprint arXiv:2010.02502*, 2020. 2
- [44] Yiren Song, Shijie Huang, Chen Yao, Xiaojun Ye, Hai Ci, Jiaming Liu, Yuxuan Zhang, and Mike Zheng Shou. Processpainter: Learn painting process from sequence data. *arXiv preprint arXiv:2406.06062*, 2024. 2
- [45] Luming Tang, Menglin Jia, Qianqian Wang, Cheng Perng Phoo, and Bharath Hariharan. Emergent correspondence from image diffusion. *Advances in Neural Information Processing Systems*, 36:1363–1389, 2023. 2, 3
- [46] Hugging Face Team. Stable diffusion reference implementation, 2023. Available online. 2, 5
- [47] Linrui Tian, Qi Wang, Bang Zhang, and Liefeng Bo. Emo: Emote portrait alive-generating expressive portrait videos with audio2video diffusion model under weak conditions. *arXiv preprint arXiv:2402.17485*, 2024. 5
- [48] Haofan Wang, Matteo Spinelli, Qixun Wang, Xu Bai, Zekui Qin, and Anthony Chen. Instantstyle: Free lunch towards style-preserving in text-to-image generation. *arXiv preprint arXiv:2404.02733*, 2024. 3, 6
- [49] Qixun Wang, Xu Bai, Haofan Wang, Zekui Qin, and Anthony Chen. Instantid: Zero-shot identity-preserving generation in seconds. *arXiv preprint arXiv:2401.07519*, 2024. 3
- [50] Sheng-Yu Wang, Alexei A. Efros, Jun-Yan Zhu, and Richard Zhang. Evaluating data attribution for text-to-image models. In *ICCV*, 2023. 3
- [51] You Xie, Hongyi Xu, Guoxian Song, Chao Wang, Yichun Shi, and Linjie Luo. X-portrait: Expressive portrait animation with hierarchical motion attention. In *ACM SIGGRAPH 2024 Conference Papers*, pages 1–11, 2024. 5
- [52] Zhongcong Xu, Jianfeng Zhang, Jun Hao Liew, Hanshu Yan, Jia-Wei Liu, Chenxu Zhang, Jiashi Feng, and Mike Zheng Shou. Magicanimate: Temporally consistent human image animation using diffusion model. In *Proceedings of the IEEE/CVF Conference on Computer Vision and Pattern Recognition*, pages 1481–1490, 2024. 2, 3, 5

- [53] Hu Ye, Jun Zhang, Sibao Liu, Xiao Han, and Wei Yang. Ip-adapter: Text compatible image prompt adapter for text-to-image diffusion models. *arXiv preprint arXiv:2308.06721*, 2023. [2](#), [3](#), [5](#)
- [54] Hu Ye, Jun Zhang, Sibao Liu, Xiao Han, and Wei Yang. Ip-adapter: Text compatible image prompt adapter for text-to-image diffusion models. *arXiv preprint arXiv:2308.06721*, 2023. [3](#)
- [55] Guanqi Zhan, Chuanxia Zheng, Weidi Xie, and Andrew Zisserman. A general protocol to probe large vision models for 3d physical understanding. In *The Thirty-eighth Annual Conference on Neural Information Processing Systems*, 2023. [2](#)
- [56] Lvmin Zhang and Maneesh Agrawala. Adding conditional control to text-to-image diffusion models. *arXiv preprint arXiv:2302.05543*, 2023. [2](#)
- [57] Richard Zhang, Phillip Isola, Alexei A Efros, Eli Shechtman, and Oliver Wang. The unreasonable effectiveness of deep features as a perceptual metric. In *Proceedings of the IEEE conference on computer vision and pattern recognition*, pages 586–595, 2018. [3](#), [6](#), [7](#)
- [58] Shiwei Zhang, Jiayu Wang, Yingya Zhang, Kang Zhao, Hangjie Yuan, Zhiwu Qin, Xiang Wang, Deli Zhao, and Jingren Zhou. I2vgen-xl: High-quality image-to-video synthesis via cascaded diffusion models. *arXiv preprint arXiv:2311.04145*, 2023. [3](#), [5](#)
- [59] Yuxuan Zhang, Yiren Song, Jiaming Liu, Rui Wang, Jinpeng Yu, Hao Tang, Huaxia Li, Xu Tang, Yao Hu, Han Pan, et al. Ssr-encoder: Encoding selective subject representation for subject-driven generation. In *Proceedings of the IEEE/CVF Conference on Computer Vision and Pattern Recognition*, pages 8069–8078, 2024. [1](#), [3](#)
- [60] Yuxuan Zhang, Yiren Song, Jinpeng Yu, Han Pan, and Zhongliang Jing. Fast personalized text to image synthesis with attention injection. In *ICASSP 2024-2024 IEEE International Conference on Acoustics, Speech and Signal Processing (ICASSP)*, pages 6195–6199. IEEE, 2024. [3](#)
- [61] Yuxuan Zhang, Lifu Wei, Qing Zhang, Yiren Song, Jiaming Liu, Huaxia Li, Xu Tang, Yao Hu, and Haibo Zhao. Stable-makeup: When real-world makeup transfer meets diffusion model. *arXiv preprint arXiv:2403.07764*, 2024. [2](#), [3](#), [5](#)
- [62] Yuxuan Zhang, Qing Zhang, Yiren Song, and Jiaming Liu. Stable-hair: Real-world hair transfer via diffusion model. *arXiv preprint arXiv:2407.14078*, 2024. [2](#), [3](#), [5](#)

DiffSim: Taming Diffusion Models for Evaluating Visual Similarity

Supplementary Material

6. Experimental Details in Different Bench

On each benchmark, the similarity scores are computed between a reference image and two candidate images, one of which is closer to the reference image. Image pair with the higher score is selected as the choice of current evaluated model. In this section, we will explain details of reference and candidate images selection for each benchmark.

6.1. NIGHTS Dataset

NIGHTS (Novel Image Generations with Human-Tested Similarities) is a dataset comprising 20,019 image triplets with human scores of perceptual similarity. Each triplet consists of a reference image and two distortions. This paper utilizes the test set of NIGHTS, which includes 2,120 image triplets. We calculate the DiffSim score for the reference image and the two distortions separately, using human evaluation results as the ground truth.

6.2. Dreambench++ Dataset

The Dreambench++ Dataset consists of generated images created using different generation methods, along with human-rated scores for how similar each image is to the original. In our experiment, we use the original image as the reference and randomly select two generated images based on it. The one with the higher human rating is considered closer to the reference. The dataset includes a total of 937 triplets.

6.3. CUTE Dataset

The CUTE Dataset includes photos of various instances taken under different lighting and positional conditions. In our experiment, for each category, we repeat the process 10 times: randomly selecting two images of the same instance under the same lighting and one image of a different instance under the same lighting. The two images of the same instance are considered more similar. The dataset contains a total of 1,800 triplets for comparison.

6.4. IP Bench

IP Bench contains 299 character classes, each with an original image and six variations generated using different consistency weights. In our experiment, we repeat the process for 5 times: using the original image as the reference and randomly selecting two generated images from the same class. The image with the higher consistency weight is considered closer to the reference. There are a total of 1,495 triplets for comparisons.

6.5. TID2013 Dataset

The TID2013 dataset contains 25 reference images, each distorted using 24 types of distortions at 5 different levels. In our experiment, we use a reference image as the starting point and randomly select two distorted images using the same type of distortions from the same reference. The image with a lower distortion level is considered closer to the reference. There are a total of 600 triplets for evaluation.

6.6. Sref Dataset

The Sref bench includes 508 styles manually selected by artists and generated by Midjourney, with each style featuring four images. When constructing image triplets, we randomly select two images from the same style and one image from a different style. We fix the random seed to construct 2,000 image triplets for quantitative evaluation.

6.7. InstantStyle Bench

The InstantStyle bench includes 30 styles, with each style comprising five images. When constructing image triplets, we randomly select two images from the same style and one image from a different style. We fix the random seed to construct 2,000 image triplets for quantitative evaluation.

6.8. TikTok Dataset

For tiktok dataset, we extract 10 frames from each video, and calculate the variance of different similarity metric scores between the first frame and other frame. A lower variance indicates that the metric demonstrates better robustness to changes in the movements of characters in the video.

7. Exploring Different Model Architectures

In Table 5, we present the performance differences of DiffSim using pre-trained models with different architectures. DiffSim-S SD1.5 leads in all benchmarks except for the CUTE dataset. DiffSim-C SD1.5 performs better on the CUTE dataset, possibly because the cross-attention layers in the U-Net architecture are particularly effective at distinguishing the subject. On the other hand, DiffSim-C uses IP-Adapter Plus, and the CLIP image encoder may become a performance bottleneck in other benchmarks. Models with higher resolution, such as SD-XL and DIT-XL/2 512, do not show performance improvement compared to lower resolution models like SD1.5 and DIT-XL/2 256. Furthermore, the performance of models using DIT as the pre-trained model is worse than using U-Net, with two possible reasons: 1. DIT splits the image into patches and then serial-

Table 5. Performance of diffsim across various benchmarks with different pre-trained models. Best results are highlighted in bold.

Model / Benchmark	Human-align Similarity		Instance Similarity		Low-level Similarity	Style Similarity	
	NIGHTS	Dreambench++	CUTE	IP	TID2013	Sref	InstantStyle bench
DiffSim-S SD1.5	86.52%	71.50%	72.06%	92.04%	94.17%	97.40%	99.05%
DiffSim-C SD1.5	79.16%	67.45%	76.17%	77.06%	94.00%	94.70%	95.10%
DiffSim-S SD-XL	78.05%	63.93%	69.94%	83.41%	91.33%	93.05%	96.55%
DiffSim DIT-XL/2 256	63.38%	57.52%	53.44%	82.81%	83.50%	77.00%	80.15%
DiffSim DIT-XL/2 512	67.92%	57.31%	57.22%	81.00%	88.67%	78.20%	79.40%

izes them, which may lead to the loss of spatial information, which is detrimental to DiffSim, despite the use of positional encoding. 2. DIT is trained on the ImageNet dataset, which is much smaller than the SD1.5 and SD-XL models' training datasets.

8. Additional Experimental Results

In Figures 7 to 13, we present the default implementation of DiffSim, which is based on the self-attention layers of SD1.5, showing results across different layers and denoising time steps t .

9. Additional Visual Examples

Figure 14 and 15 show more examples of images from Sref bench and IP bench; Figure 16 presents more top-4 retrieval results of DiffSim, CLIP, DINO v2 on MS COCO, Sref bench and IP bench.

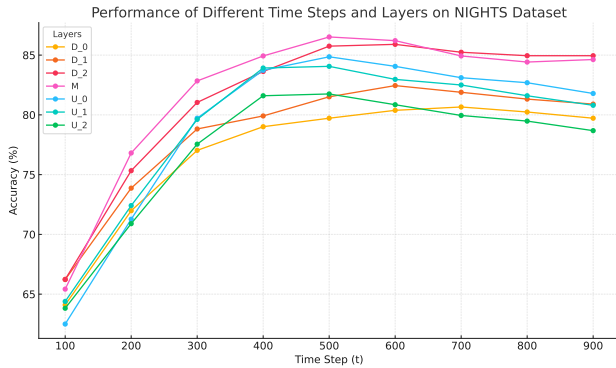


Figure 7. Results on NIGHTS dataset.

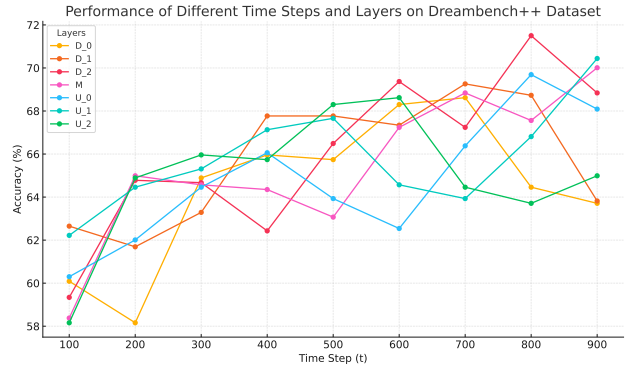


Figure 8. Results on Dreambench++ dataset.

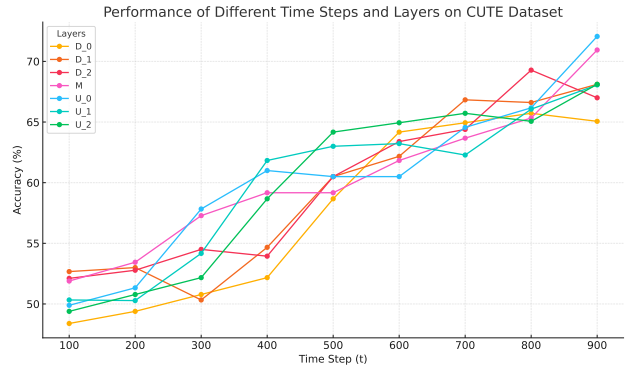


Figure 9. Results on CUTE dataset.

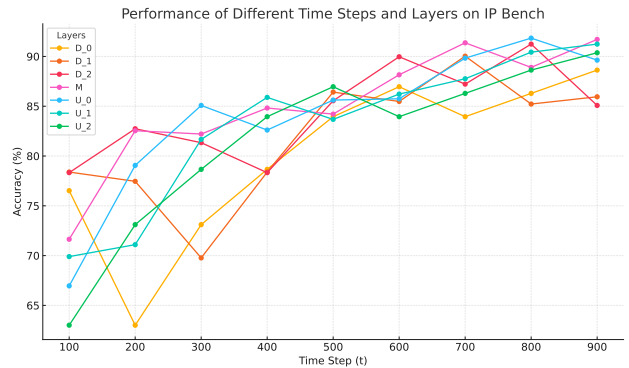


Figure 10. Results on IP bench.

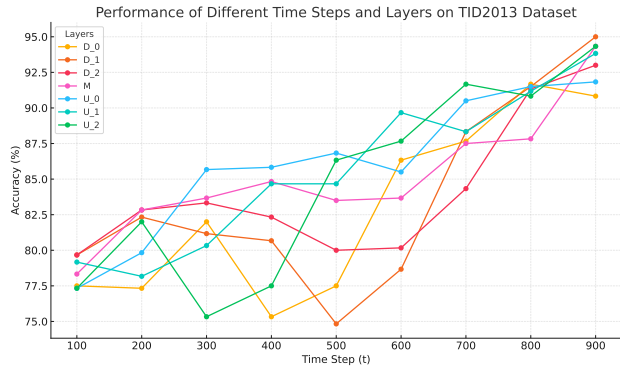


Figure 11. Results on TID2013 dataset.

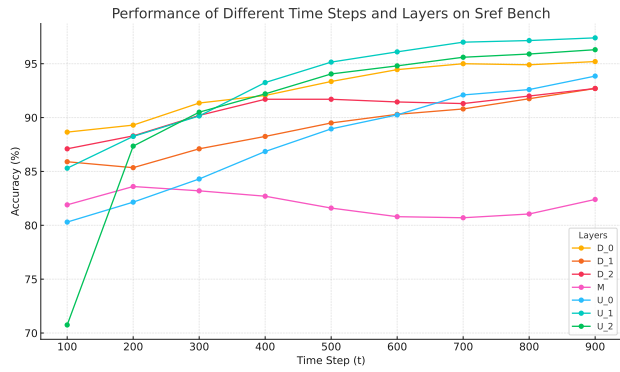


Figure 12. Results on Sref bench.

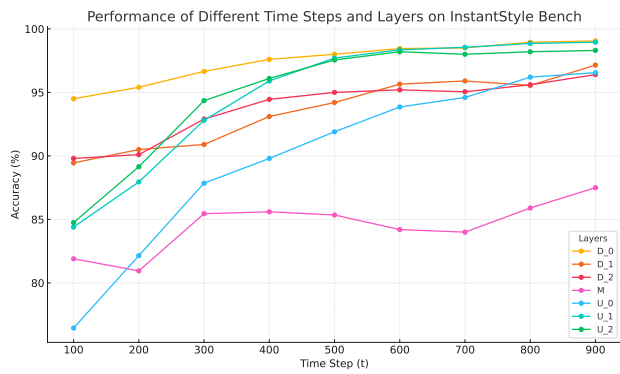


Figure 13. Results on InstantStyle bench.

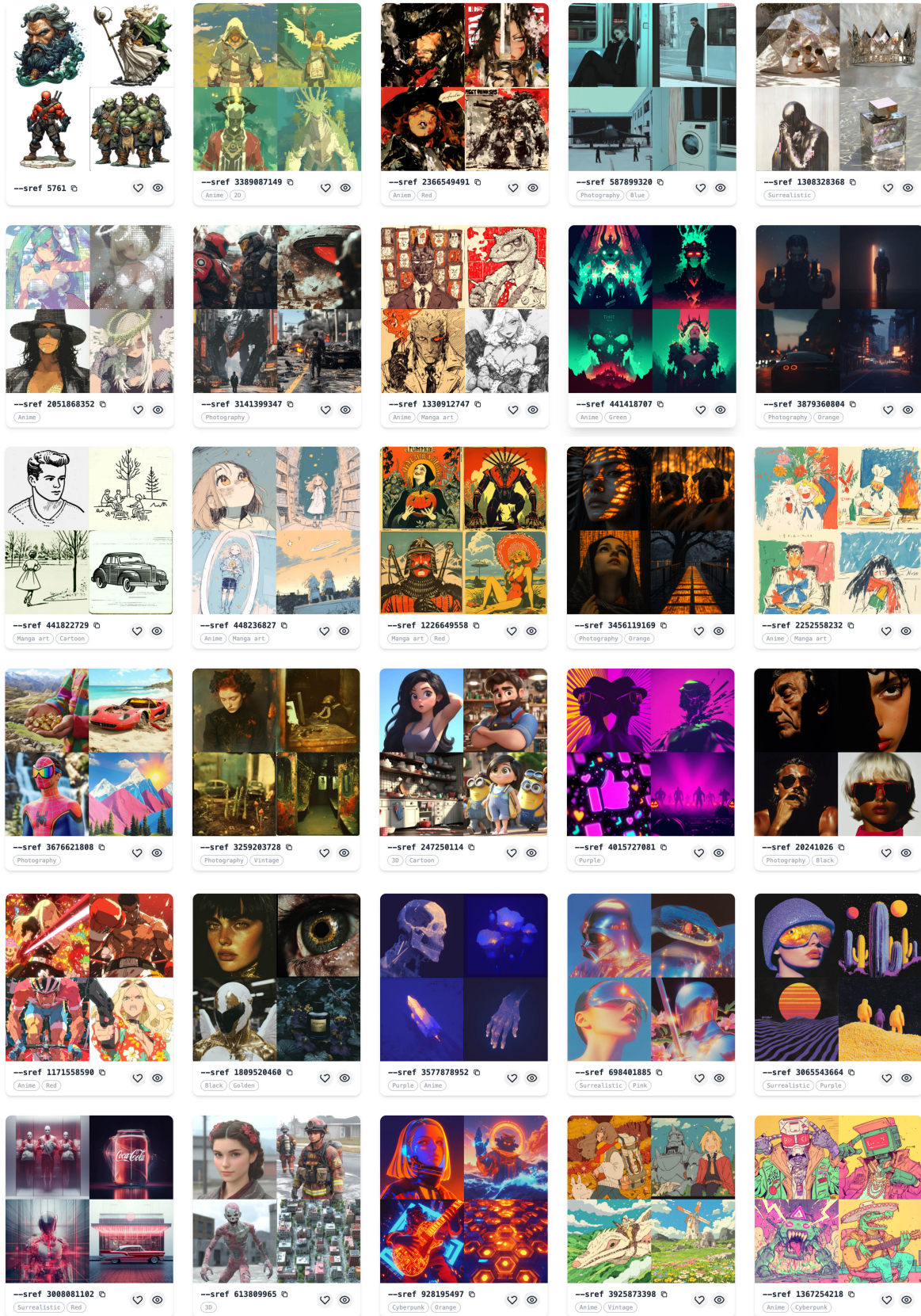


Figure 14. Examples in Sref bench we proposed.

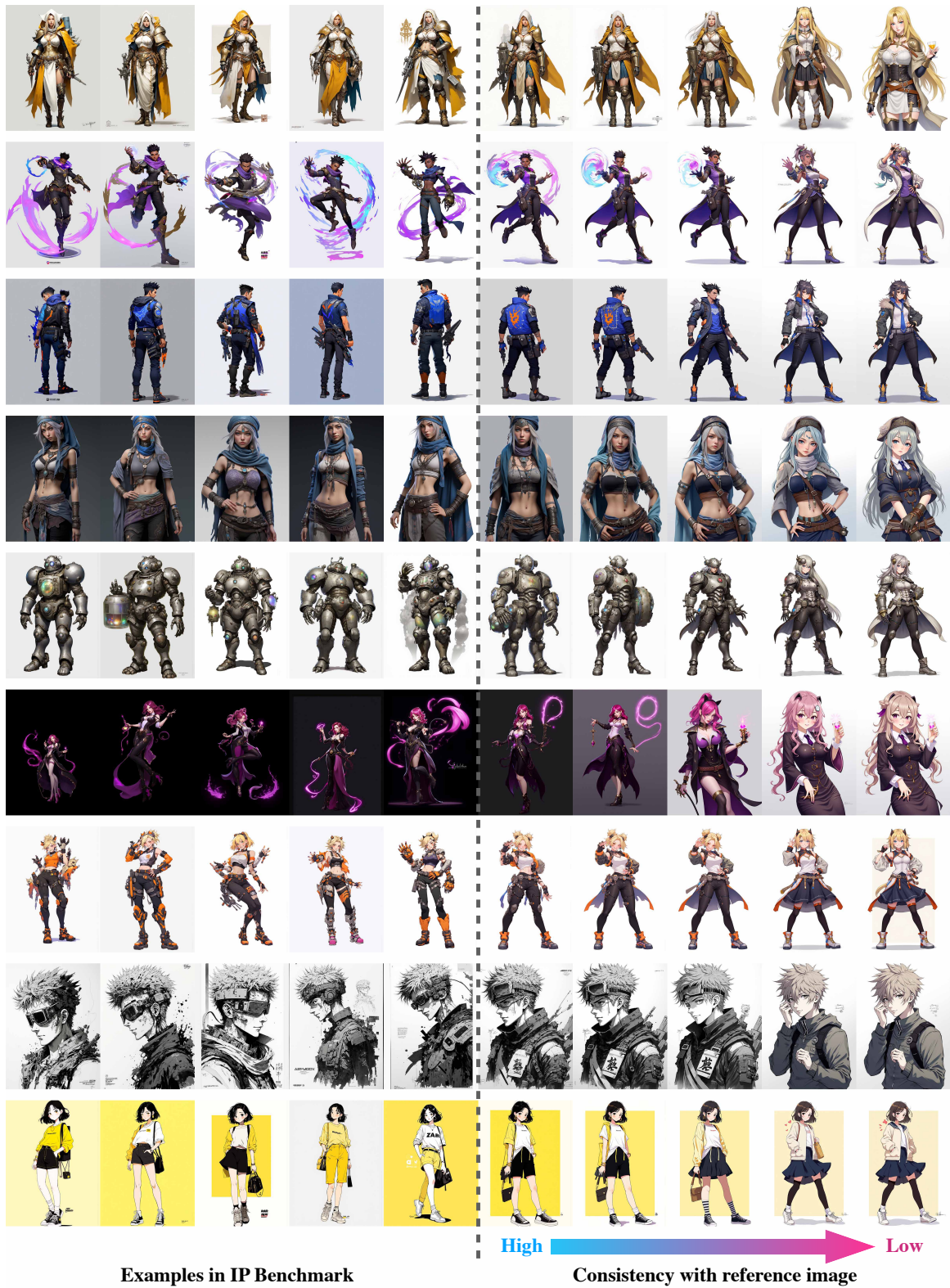


Figure 15. Examples in IP bench we proposed.

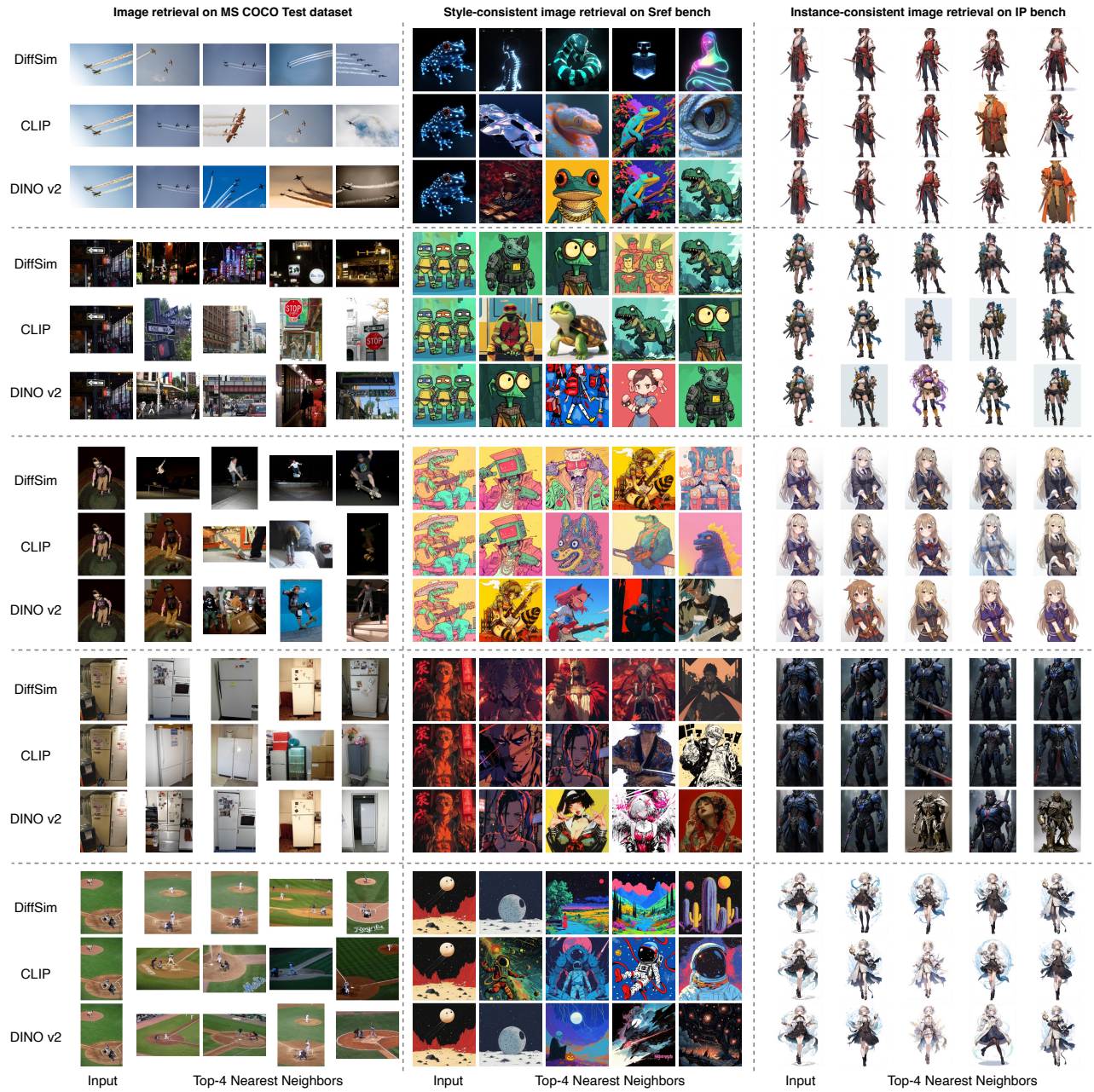


Figure 16. More image retrieval results.